THE PENNSYLVANIA
STATE UNIVERSITY

# IONOSPHERIC RESEARCH

Scientific Report No. 329(E)

## PULSE CIRCUITRY FOR A FLYABLE TIME-OF-FLIGHT MASS SPECTROMETER

by
R. B. Hazelton
December 10, 1968



IONOSPHERE RESEARCH LABORATORY

University Park, Pennsylvania NASA Grant NGR 39-009-032

IONOSPHERIC RESEARCH

NASA Grant NGR39-009-032

Scientific Report

on

# "Pulse Circuitry for a Flyable Time-of-Flight Mass Spectrometer"

by

R. B. Hazelton

December 10, 1968

Scientific Report No. 329(E)

Ionosphere Research Laboratory

Submitted by: B. R. F. Kendall (AW)
B. R. F. Kendall, Associate Professor of Physics

Approved by: A. H. Waynick
A. H. Waynick, Professor of Electrical Engineering
Director, Ionosphere Research Laboratory

The Pennsylvania State University

College of Engineering

Department of Electrical Engineering

TABLE OF CONTENTS

# ABSTRACT

The development of pulse circuitry for a time-of-flight mass spectrometer is described. A method is presented for electronically sweeping the delay time between two pulses in order to provide sampling of the spectrometer's ion beam. This results in shifting the information content of the instrument's output to lower frequencies thus allowing the spectrometer to be used with simpler dc electrometer circuits. The circuitry was designed with emphasis on low power consumption and other factors which are desirable for rocket probes. Practical pulse and timing techniques are presented which may prove useful in other areas involving pulse circuitry.

# CHAPTER I

# INTRODUCTION

## 1.1 The Linear Time-of-Flight Mass Spectrometer

The principle of the time-of-flight mass spectrometer was first presented by Stephens[1]. In its simplest form the linear time-of-flight instrument consists of two grids and a plate as shown in Figure 1. Positive ions in region A are accelerated toward the collector by a positive pulse on grid 1. Assuming the ions are all given the same energy, the lighter ions will possess a greater velocity than the heavier ones and will arrive at the collector first. A third grid placed just in front of the collector keeps the collector from developing an image charge as the ions approach. Electrons flow to the collector through the collector resistor $R_1$ to neutralize the positive ions as they hit the collector. Since this electron current is a reproduction of the ion current, a method used to observe the resulting mass spectrum is to amplify the voltage drop across $R_1$ and apply it to the vertical amplifier of an oscilloscope. The trace of the oscilloscope would be swept horizontally by the internal time-base which would be triggered by the pulse to grid 1. A timing sequence is shown for illustration in Figure 2. The output current shows the presence of two low mass ions and a third heavier species of relatively low concentration.

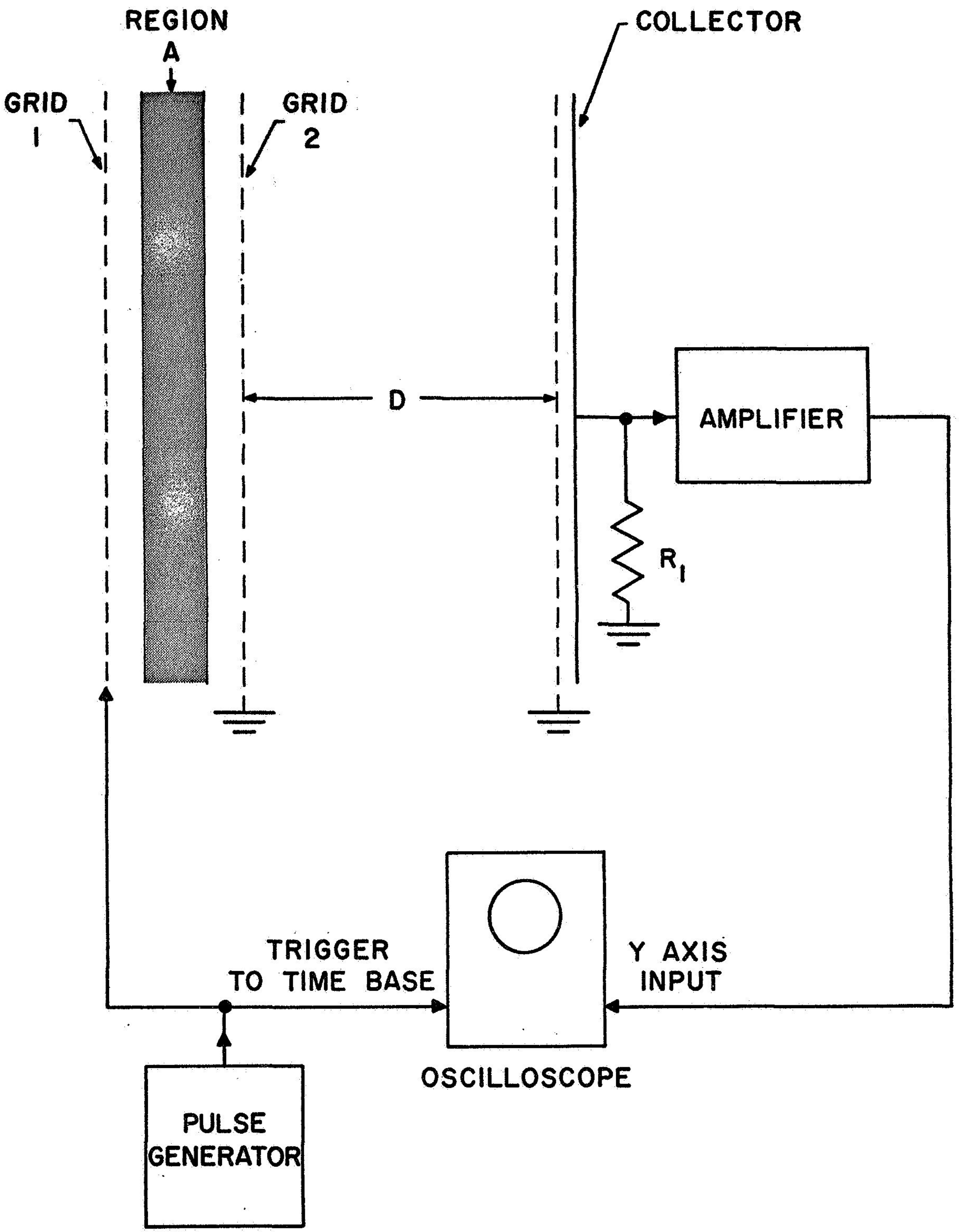


BASIC TIME-OF-FLIGHT MASS SPECTROMETER

FIGURE 1

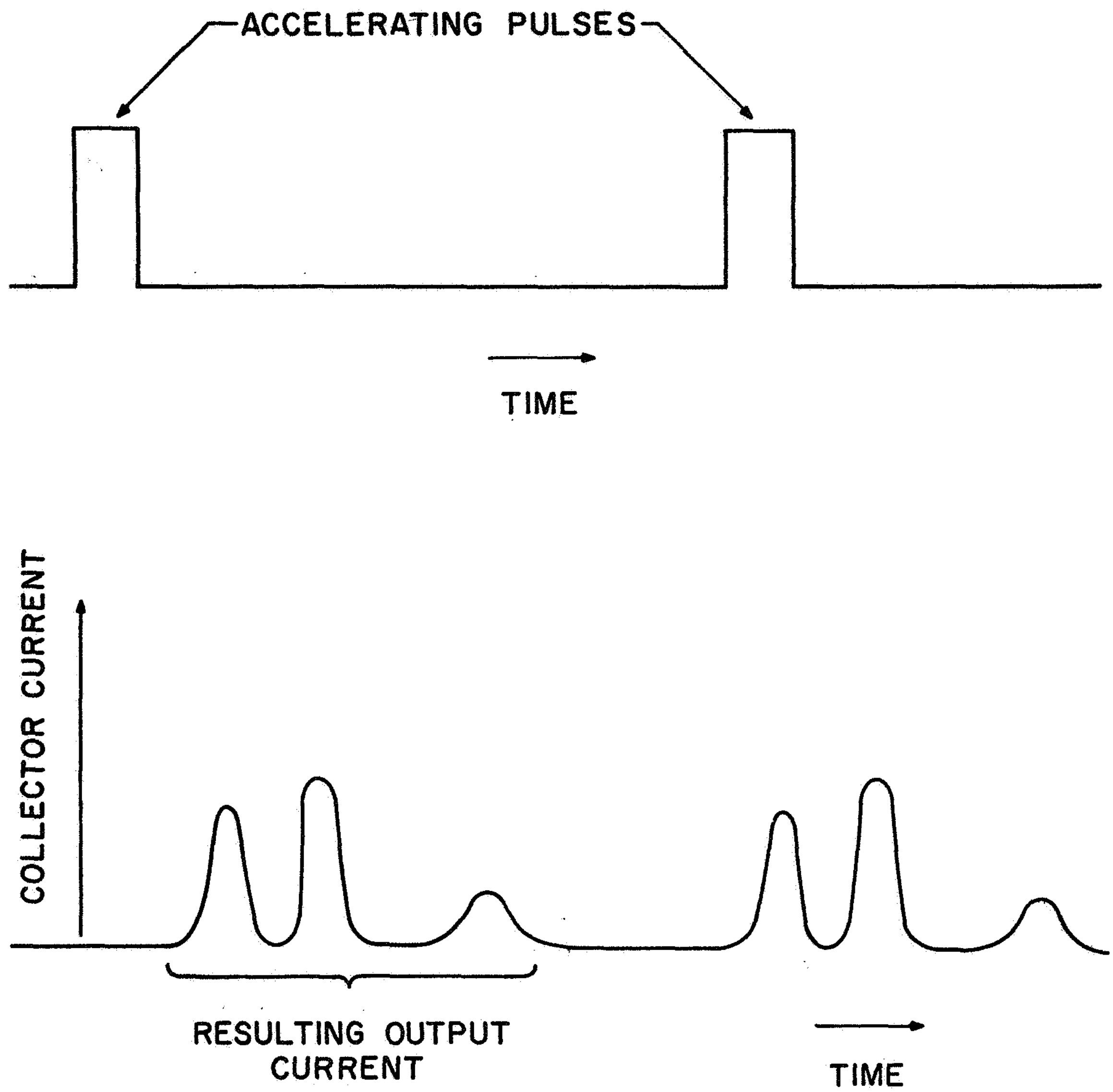


ACCELERATING PULSES AND RESULTING OUTPUT FROM THE TIME-OF-FLIGHT INSTRUMENT

FIGURE 2

## 1.2 The Linear Instrument with Space Focusing

Wiley and McLaren[2] redesigned the linear time-of-flight mass spectrometer by placing two distinct accelerating areas in the source region as shown in Figure 3. The voltages on the electrodes which bound the two accelerating regions can be adjusted such that an ion in region A initially closer to the pulsed grid will receive enough additional energy to reach the collector at the same time as an ion of the same mass also in region A which is initially closer to the collector. This results in increasing the ability of the instrument to detect the presence of two ion species which differ by only a few mass units. Wiley and McLaren's actual instrument was similar to that shown in Figure 3 with the exception of an electron multiplier used to measure the ion current.

## 1.3 The Time-of-Flight Mass Spectrometer - Practical Considerations

Generally speaking the following relationships involving sensitivity, resolution and size apply to the time-of-flight mass spectrometer:

1. If a singly charged ion is subjected to an accelerating potential V measured with respect to ground, its velocity when in a grounded flight region will be related to its mass by

$$eV = \frac{1}{2} mv^2 \qquad (1)$$

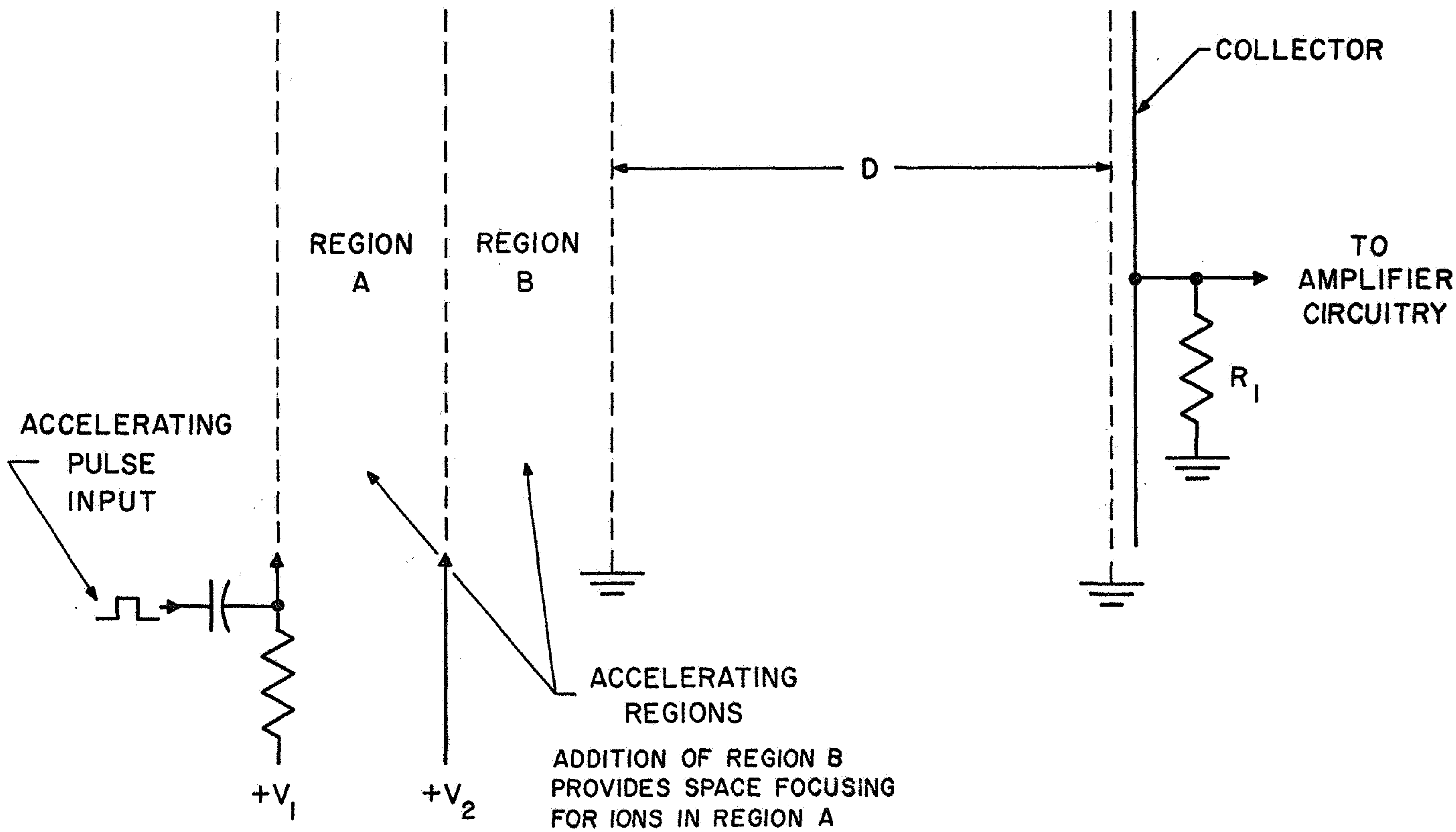


TIME-OF-FLIGHT MASS SPECTROMETER WITH SPACE FOCUSING

FIGURE 3

For a flight length D, the approximate time that it will take for an ion to reach the collector after the accelerating pulse has been applied is found by applying equation (1) with

$$v = \frac{D}{t} \tag{2}$$

yielding

$$eV = \frac{1}{2} m\left(\frac{D}{t}\right)^2 \tag{3}$$

This rearranges into equation (4).

$$t_{(usec)} = 0.7D_{(cm)} \sqrt{\frac{m(\text{Atomic Mass Units})}{V(\text{Volts})}} \tag{4}$$

2. The longer the flight length D, the greater the time between corresponding mass peaks. This in itself is not a change in resolution but can result in an improvement in resolution if the circuitry associated with the collector does not have sufficient frequency response and tends to smear the mass peaks together.

3. The longer the flight length, the greater the possibility of molecular collisions. Therefore instruments with long flight paths must be used at low pressures to preserve instrument sensitivity and resolution.

4. If region A is made larger, a greater number of ions will be pulsed and therefore the sensitivity of the instrument will be increased.

5. Relative ion concentrations are obtained by measuring the relative ion current peak heights. Absolute ion concentrations can also be obtained by utilizing more complex methods of analysis.

The above considerations applied to the problem of measuring and identifying ions in the ionosphere utilizing rocket probes has led to the use of the wedge time-of-flight mass spectrometer[3]. The wedge instrument is actually a sector of a circular time-of-flight instrument. The circular geometry has the advantage of having a large accelerating region for its size.

## 1.4 The Wedge Time-of-Flight Mass Spectrometer

The basic wedge time-of-flight instrument is shown in Figure 4. Positive ions are drawn toward the spectrometer by a negative potential on grid 1. Grid 2 is placed at ground or a slightly positive potential to ensure the ions are decelerated enough such that they do not enter region B and that the energy of the ions in region A remains small. A high positive pulse on grid 1 accelerates the ions from region A into region B. A constant negative potential on grid 3 further accelerates the ions toward the collector. The two regions comprise a Wiley-McLaren source in a cylindrical form. The third region, the flight region, must have no voltage gradient across it, hence grid 3 and grid 4 are connected together. For the same reason plates 1 and 2 are added on the sides and connected to grids 3 and 4. Grids 4, 5 and 6 comprise a gating system which will be discussed in section 1.6.

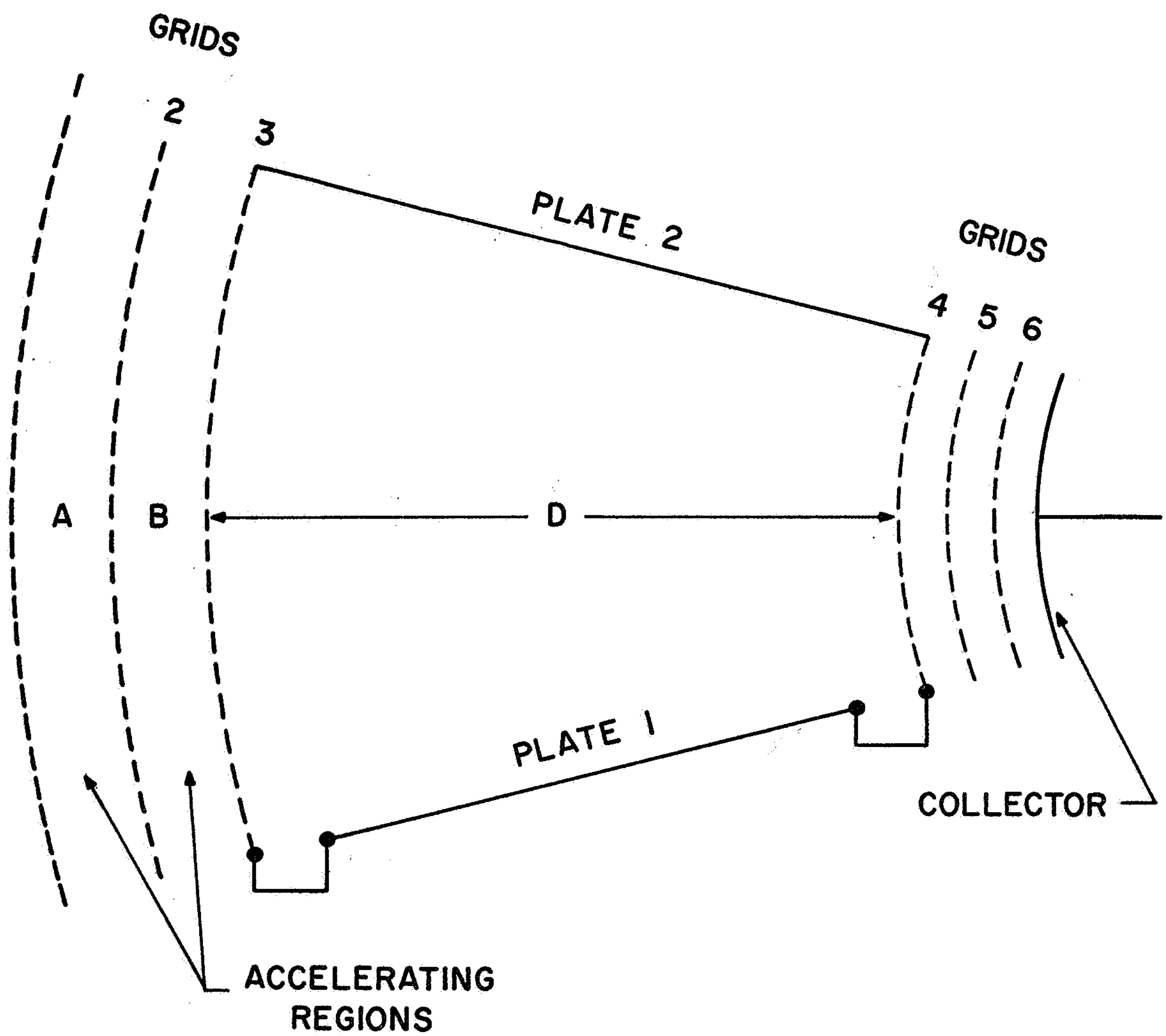


GEOMETRY OF THE WEDGE
TIME-OF-FLIGHT INSTRUMENT

FIGURE 4

## 1.5 The Electronic Specifications of the Wedge Instrument

The actual grid voltages, pulse height and pulse width depend upon the exact geometry of the spectrometer. Experiments are being conducted concurrently to establish the exact potentials for best instrument sensitivity and resolution. Preliminary experiments have shown that reasonable performance should occur with approximately -5 volts on grid 1, with pulses up to about +80 volts for approximately 2 usec. Because it is not easy to build a low energy ion source to simulate the ion energies expected during the actual rocket flight, the lab version has all its biases shifted such that the net result is that the effective ion energies are low as the ions enter accelerating region A. The rocket body is used as a reference for all voltage measurements.

The time between accelerating pulses must be enough to allow region A to refill. This required time depends upon how the instrument is flown. If the instrument is flown with its accelerating grid looking out the front of the rocket, it will refill more rapidly than if the accelerating grid "looks" out the side of the rocket. Based upon the expected rocket speeds these filling times correspond to accelerating pulse rates on the order of 50 kHz and 5 kHz.

Provisions are made to allow the second grid to be varied in potential from 0 to +5 volts. Similarly the potential on the third grid is adjustable from -55 to -65 volts. Grid 4 must also be biased at the same potential to avoid acceleration in the flight region. These voltages are optimized for the 5 mm and 3 mm widths of regions A and B, and for a flight length of 4.4 cm.

The stability requirements of the bias potentials are not exactly known. Preliminary experiments indicate that noise and instability should be kept to within 1%. This is also true of the accelerating pulse. It should be essentially "flat" on top. The risetime of the accelerating pulse should theoretically be zero. Actual practice indicates a risetime of 60 nsec or less is tolerable. The decay time, however, is not critical. After the ions have been accelerated out of region A the accelerating pulse will have no effect on them. Thus the decay time of the accelerating pulse can be quite long. The only important point is that the accelerating pulse should be of constant amplitude while it is actually accelerating the ions. The 2 usec pulse width gives sufficient time to clear the ions up to a few hundred mass units from region A.

## 1.6 Sampling to Reduce the Frequency of the Output

The collector end of such a short time-of-flight spectrometer poses many problems. A short flight length means short flight times and hence a collector current of rather high frequency components. The actual useful frequency components possibly are as high as 10 mHz for an instrument this small. In addition the average collector currents expected when the instrument is used for ionosphere measurements may be as low as $10^{-13}$ amps. Normally such low currents are amplified to more useful voltage levels by using a form of operational amplifier called an electrometer. The gain of such an amplifier is normally given by

$$\frac{V_{out}}{I_{in}} = - R_F \qquad (5)$$

where $R_F$ is the feedback resistor placed between the input and output terminals of a high gain inverting amplifier. Equation 5 is derived from the circuit shown in Figure 5 with the capacitances neglected. For high frequencies, especially at high gains ($R_F$ on the order of $10^7\Omega$ and higher), the capacitive effects are no longer negligible. Some however can be minimized or compensated for. For instance, the loss of gain due to $C_1$ can be minimized by increasing the open loop gain of the amplifier. The effects of $C_2$ can be minimized by designing the amplifier with the lowest possible output impedance. The effects of $C_3$ can be compensated for by inserting a series resistor and capacitor to ground at point A. The loss of gain due to the distributed capacitance, $C_{Dist}$, along $R_F$ is left as the limiting factor although it is possible to minimize the distributed capacitance. The presence of $C_{Dist}$ can be visualized as acting as an undesirable high frequency compensation. With the present state of the art it is possible to construct an electrometer which is useful in

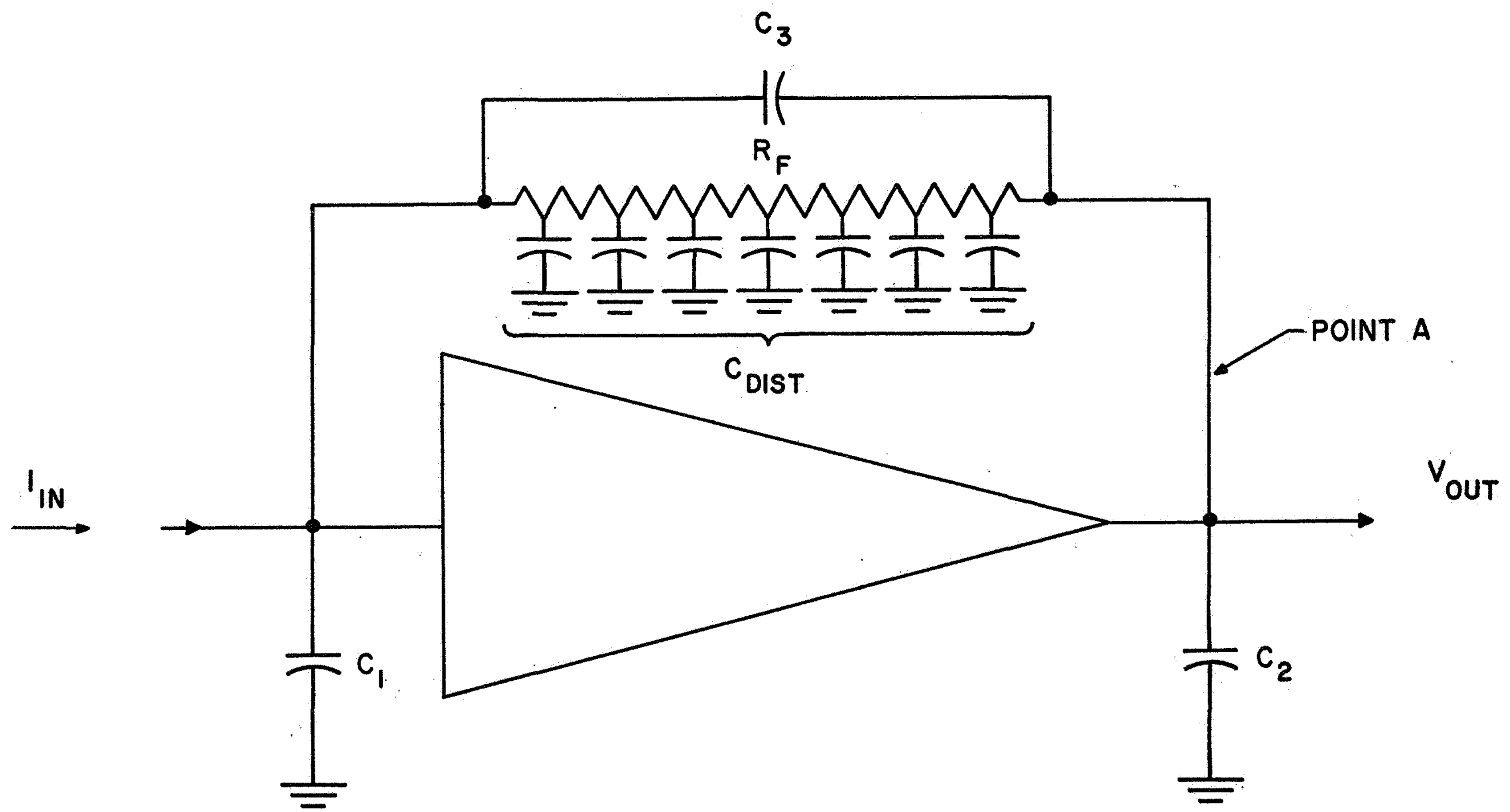


OPERATIONAL AMPLIFIER USED AS AN ELECTROMETER
SHOWING UNAVOIDABLE CAPACITANCES

FIGURE 5

the $10^{-13}$ amp range with a bandwidth up to about 1 kHz. It should also be noted that the maximum bandwidth of the commercially available telemetry channel is also 1 kHz. The solution is to implement a sampling technique to reduce the bandwidth of the signal before the ions reach the collector. Since the actual output spectrum will change very little from one accelerating pulse to the next even at rocket speeds, a sampling technique is theoretically possible. Wager(4) used a similar technique of sampling with a time-of-flight mass spectrometer rocket probe, but sampled after the electrometer amplifier. The particular spectrometer Wager was concerned with needed an electrometer with a 2 mHz bandwidth and a transresistance of 4 mV output for $10^{-7}$ amps of collector current. The actual device had a bandwidth of 860 kHz which was apparently considered usable. Gating was done after the electrometer to reduce the frequency components to a range that the telemetry could handle.

The gated collector system reduces the bandwidth requirement of the electrometer amplifier. A gating system operating ideally will have less resolution capability than the same instrument without such gating, simply because a finite gating time is required. Katzenstein and Friedland(5) were able to show experimentally that an enhancement in the signal to noise ratio could be obtained as theory predicts by gating the ions before they reach the collector.

The gating in the wedge instrument is accomplished by using three grids placed in front of the collector as shown in Figure 4. Grid 4 is kept at the same potential as grid 3 to keep the flight region field free. Similarly grid 6 is used to keep the actual gating grid, grid 5, from producing a field in the collector area. The potential on grid 5 is normally kept slightly higher than the potential of the initial accelerating pulse thus keeping the ions from reaching the collector. A narrow negative pulse applied to this grid will allow those ions which are just in front of the gating grid to pass on to the collector. Ions of other heavier species will not reach the collector because the gating grid will be back to its normal high potential by the time the ions reach the gating grid area. Lighter ions would have arrived before the gating pulse occurred and would also not reach the collector. By sweeping the gating pulse in time in relation to the accelerating pulse the entire mass spectrum will be traced out onto the collector. The frequency components of the collector current are then dependent on how rapidly the position of the gating pulse is swept through its range.

The gating pulse must be narrow, on the order of 100 nsec. Maximum output from a single ion species will occur when the gating pulse has the same width as the ion species. The actual width of an ion species is not only a function of its mass number, but is also dependent on the range of energies the ions of that species had before being drawn into the accelerating region, the spacing between grids 4 and 5, and their velocity in the gating region. A gating pulse wider than one species will broaden the peak resulting in a loss of resolution. A narrower gating pulse will result in a loss in sensitivity.

The gating grid voltage is held to +30 volts and the gating pulse has an amplitude of around -100 volts. Because of the short flight length, the lighter ions arrive at the gating area almost immediately after the accelerating pulse has occurred. To observe the heaviest ions of interest the gating pulse must be able to sweep out to approximately 6 usec from the leading edge of the accelerating pulse.

It is desirable to sweep up (or down) the mass scale in about $2\frac{1}{2}$ seconds and then sweep down (or up) in about $\frac{1}{2}$ second. The two different sweep times may yield some information about the rocket's spin in relation to ion collection. In either case the sweep will be slow enough to reduce the frequency components of the collector output to below 1 kHz.

# CHAPTER II

## METHODS OF OBTAINING THE PULSE AND TIME SEQUENCING

### 2.1 Utilizing Two Ramp Generators

There are two basic methods of obtaining the pulse and time sequencing for the gated wedge time-of-flight mass spectrometer. The most common method used with a gated time-of-flight instrument is shown in Figure 6. This scheme, basically used by Wager, compares the outputs of two ramp generators. When their outputs have the same amplitude a gating pulse is produced. Triggering from the faster generator is used to produce the accelerating pulse. This can be done directly by simply amplifying, as shown in Figure 6, if the ramp is generated by using an integrator and comparator. However, the resulting timing sequence, Figure 7, would not allow the gating pulse to sweep "under" the accelerating pulse. Since it is necessary to be able to do this in order to observe the presence of light ions, Figure 6 would have to be modified by inserting a monostable multivibrator at point A. This would be adjusted for the required delay time and its output would be used to trigger a second monostable multivibrator. The second monostable's output would be adjusted for the required 2 usec accelerating pulse width and fed into the amplifier.

### 2.2 Using a Voltage Controlled Monostable Multivibrator

A second method of obtaining the pulse and timing sequence for the time-of-flight instrument uses a monostable

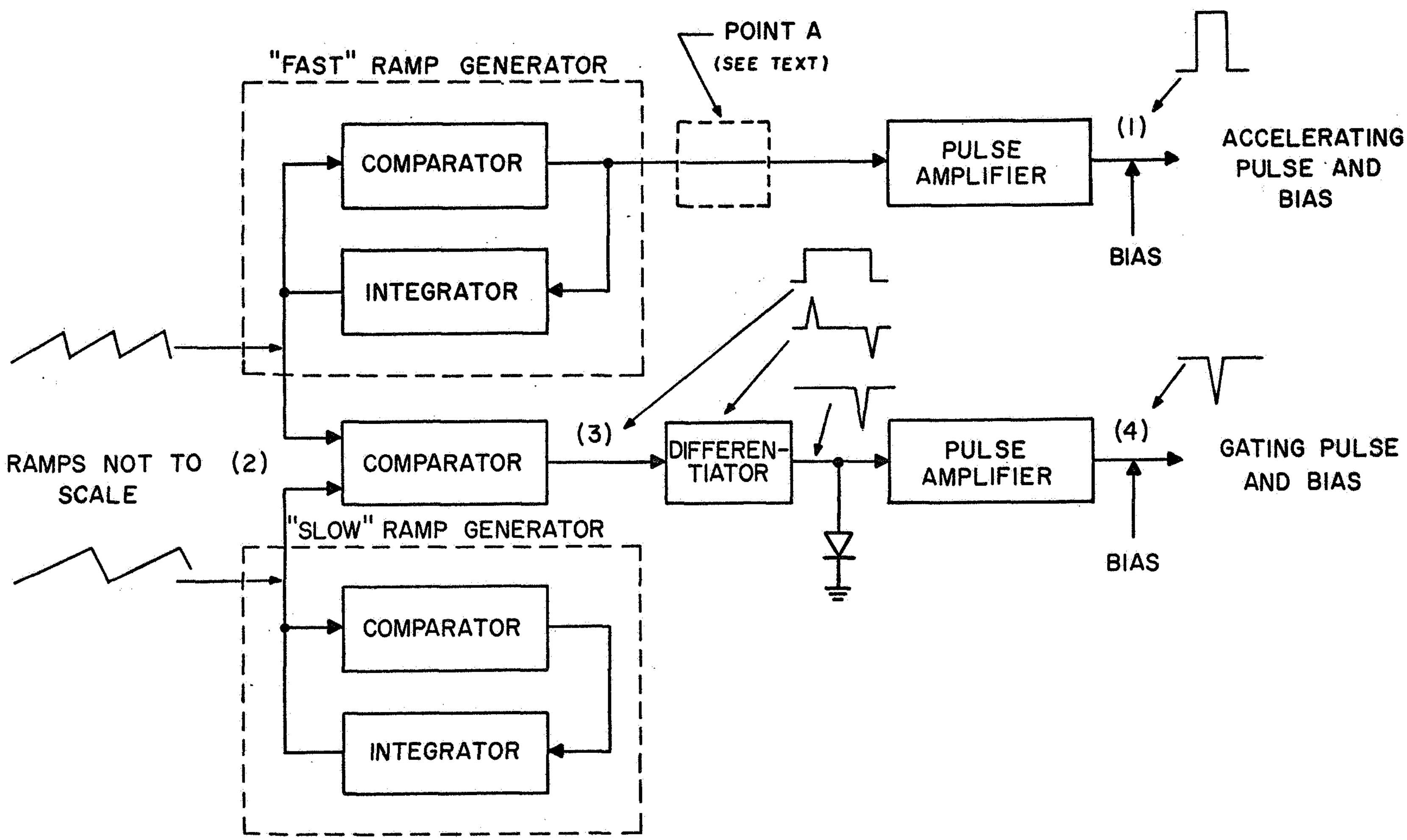


TWO-RAMP-GENERATOR APPROACH FOR PULSING THE WEDGE TIME-OF-FLIGHT MASS SPECTROMETER

FIGURE 6

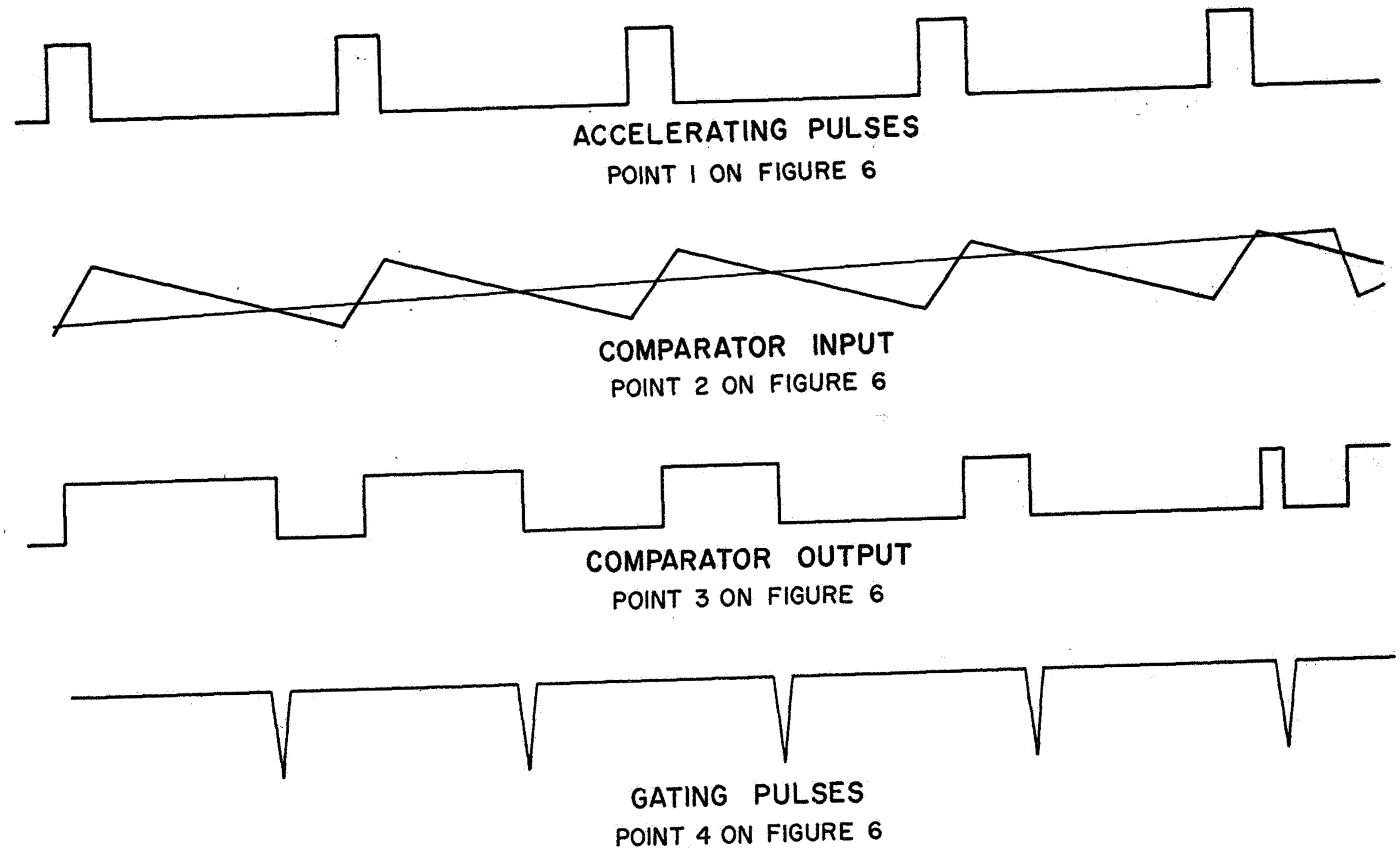


RESULTING TIME SEQUENCING OF SYSTEM OUTLINED IN FIGURE 6

FIGURE 7

multivibrator whose output pulse width has a near linear relation to the amplitude of an applied voltage. A block diagram using this approach is shown in Figure 8. The resulting timing sequence is shown in Figure 9. A free-running multivibrator is the basic timing element. Its output is amplified to produce the accelerating pulse and its leading edge is used to trigger the voltage controlled monostable multivibrator (VCMM). The width of the pulse of the VCMM is dependent upon the ramp voltage at that time. The trailing edge of the VCMM pulse is differentiated and then amplified to produce the gating pulse.

This second approach was chosen because it is easier to implement, even though the first is a more classical one.

The pulse polarities shown in Figure 8 and 9 are correct for the block diagram of Figure 8. However such a block diagram is a rather idealized system. For instance, it is more practical to build an inverting rather than a non-inverting pulse amplifier. For this and other reasons which are explained in the next chapters the actual block diagram and pulse polarities shown in Figure 17 are slightly different from those of Figure 8.

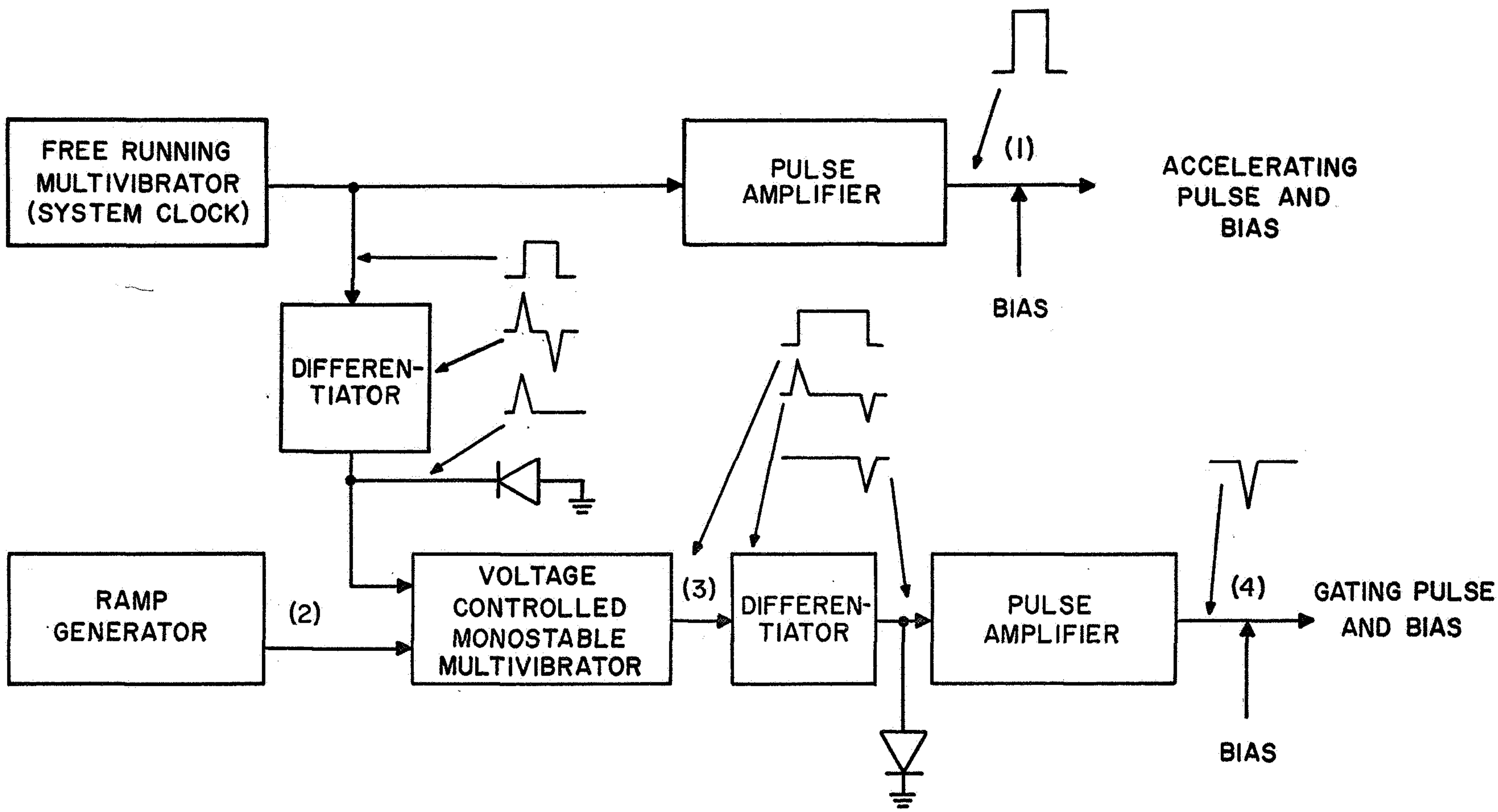


VOLTAGE CONTROLLED MULTIVIBRATOR APPROACH FOR PULSING THE WEDGE TIME-OF-FLIGHT INSTRUMENT

FIGURE 8

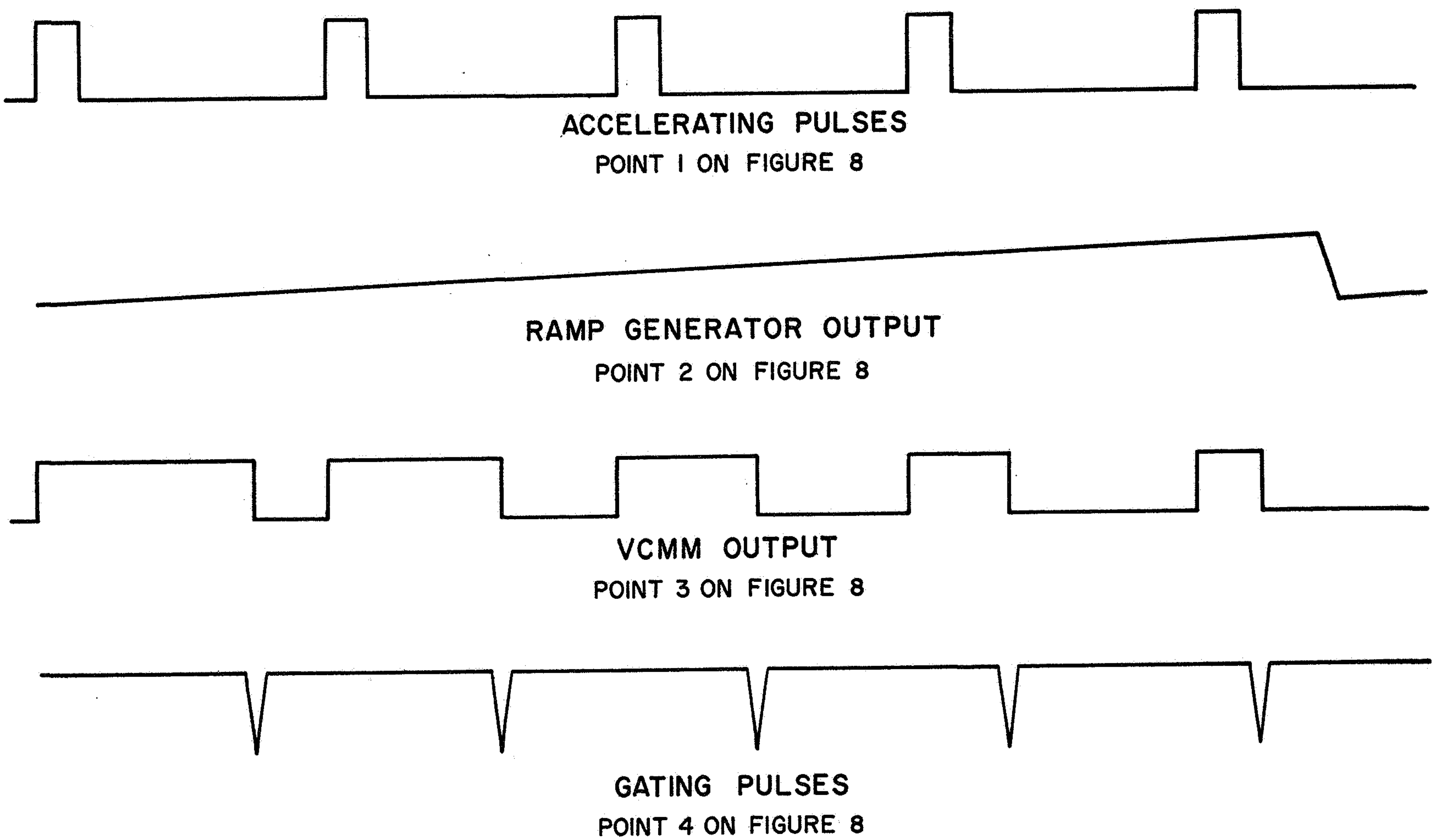


RESULTING TIME SEQUENCING OF SYSTEM OUTLINED IN FIGURE 8

FIGURE 9

# CHAPTER III

## SUPPLYING THE ACCELERATING PULSE AND BIAS

### 3.1 The System Clock

A simple free-running multivibrator is used for clocking the system at the previously mentioned 50 kHz rate with a 2 usec pulse width. To conserve power the collector resistors are kept as large as possible but not large enough to deteriorate the pulse rise time. The 2 usec "on time" and approximately 20 usec "off time" require drastically different values of $C_1$ and $C_2$. See Figure 10. Because of the heavy capacitive loading of $C_2$, the waveform on the collector of $Q_1$ is distorted to the extent that it is not a useful output. The lighter loading of $C_1$ on the collector of $Q_2$ allows the collector waveform to reach the supply voltage with a 40 nsec rise time and a 100 nsec decay time or more depending upon loading. The pulse is then fed through the decoupling network $C_3$ and $R_5$ to provide drive for the accelerating pulse amplifier, transistor $Q_3$.

### 3.2 The Accelerating Pulse Amplifier

Since the accelerating pulse amplifier contains a single transistor in a grounded emitter configuration, it will invert the negative pulse supplied by the system clock that is applied to its base and produce a positive output pulse. This is the required polarity for a positive ion time-of-flight instrument. An instrument for negative ions would have an inverting stage between the clock and the

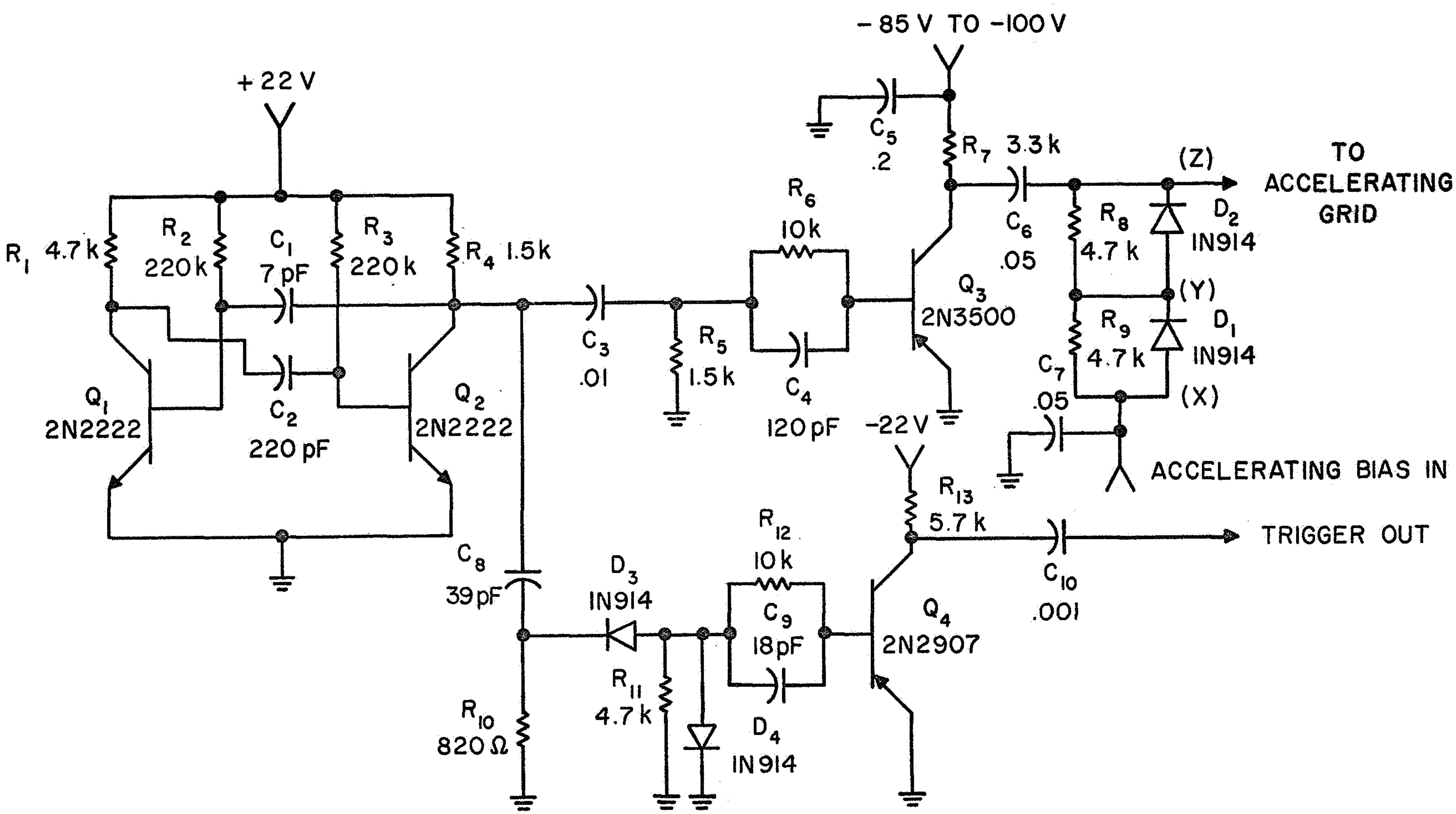


THE SYSTEM CLOCK, ACCELERATING AMPLIFIER, DIFFERENTIATOR, AND DIFFERENTIATOR AMPLIFIER

FIGURE 10

accelerating amplifier stage. It should be noted that the positive ion spectrometer is more important in the early stages of spectrometer testing since it is much easier to produce positive ions under laboratory conditions.

A PNP transistor is used for the accelerating amplifier in the positive instrument. This is done because an NPN stage would have to be pulsed off rather than on when driven by the system clock, thus power would be drawn for the 20 usec part of the cycle rather than for the 2 usec part. By using a PNP rather than an NPN stage the dissipation requirements of the transistor as well as the average power drain on the power supply are reduced.

The rise time of the accelerating pulse is determined by how quickly the base-emitter junction of $Q_3$ can be forward biased. For this reason a speed-up capacitor, $C_4$, is connected in parallel with $R_6$ to increase the coupling of the high frequency components which are contained in the leading edge thus reducing $Q_3$'s transition time. The fastest rise time that could be experimentally achieved with the 2N3500 transistor in this configuration was 60 nsec, which is sufficient. To get the fastest decay time of the accelerating pulse, a small value for $R_7$ is required. However this imposes rather high instantaneous currents on the power supply which produces ringing and appears on the pulse as a damped sine wave oscillation. Because the pulse must appear essentially flat across the top, a compromise is made by making $R_7$ large enough to reduce the ringing at the expense of the pulse decay time. However as stated earlier the decay time of the accelerating pulse is not important. Capacitor $C_5$ and a ferrite bead placed on the power supply lead helps reduce the large instantaneous current drain from the supply. The accelerating pulse is decoupled from the collector of $Q_3$ by $R_8$, $R_9$, $C_6$ and $C_7$.

## 3.3 Adding the Accelerating Bias

Bias is added to the accelerating grid through a dc restoring network consisting of $R_8$, $R_9$, $D_1$, $D_2$ and $C_7$. With no accelerating pulse present the same bias potential appears at points X, Y and Z, since current is never drawn by the accelerating grid which would produce an IR drop across $R_8$ or $R_9$. A positive pulse occurring at the collector of $Q_3$, which is ac coupled through $C_6$ has the most negative portion of its waveform clamped to the bias potential applied at the junction of $R_9$, $D_1$ and $C_7$. The net result is a normal bias potential and a pulse added to it, rather than a bias with an ac coupled pulse added to it. The two diodes and equalizing resistors are used to obtain a sufficient peak inverse rating. The actual capacitance of the grid should be taken into consideration although it was previously stated that capacitive loading was not a problem at this point since the decay time of the accelerating pulse is not important. An external load of 70 pF was connected from point Z to ground as a measure to insure that no adverse effects had occurred. The loading did lengthen the decay time, but the rise time remained approximately 60 nsec.

### 3.4 Circuit for Triggering the Voltage Controlled Monostable Multivibrator (VCMM)

In addition to driving the accelerating pulse amplifier the clock output is also differentiated and used to trigger the voltage controlled monostable multivibrator. To allow the VCMM to "sweep under" the accelerating pulse the leading edge of the clock pulse is used for the triggering. The differentiator network is comprised of $R_{10}$ and $C_8$. $C_8$ is also used for decoupling. The positive part of the derivative is filtered out by diodes, $D_3$ and $D_4$. $R_{11}$ provides a "fast" dc path for both diodes. The actual drive to the differentiator amplifier is accomplished through $R_{12}$ and a speed-up capacitor $C_9$. Again the philosophy of having the transistor turned on for the pulse part of the waveform is incorporated by using a PNP stage for the differentiator amplifier. A shield was placed between the clock and the VCMM to insure that the trailing edge of the clock pulse would not accidentally trigger the monostable. For similar reasons the accelerating pulse amplifier was placed on the side of the clock opposite the monostable circuitry.

The output pulse from the differentiator amplifier has a height of eight volts and a width of 100 nsec at the zero volt level. This proves to be sufficient to provide reliable triggering to the monostable multivibrator.

It should be noted that 22 volts was chosen for the supply voltage for the clock, because that much voltage is needed to drive the differentiator and still have enough amplitude to reliably turn on $Q_4$. A -22 volt supply was also used since a similar situation exists in other parts of the circuitry requiring a negative supply. Because the pulses are a.c. coupled throughout the circuitry it would be possible to operate all the stages from a single supply.

# CHAPTER IV

# THE VOLTAGE CONTROLLED MONOSTABLE MULTIVIBRATOR AND ITS RAMP DRIVE

## 4.1 The Voltage Controlled Monostable Multivibrator[6]

The voltage controlled monostable multivibrator is basically an emitter coupled multivibrator whose output pulse width is linearly dependent upon an applied voltage $V_{in}$. The circuit is shown in Figure 11.

Normally $Q_6$ is in a forward biased condition producing a seven volt drop across $R_{14}$ with the values of $R_{14}$, $R_{15}$ and $R_{16}$ shown. The maximum voltage of $V_{in}$ is restricted to less than seven volts, thus keeping the base-emitter junction of $Q_5$ reverse biased. A positive trigger pulse applied through $C_{10}$ forward biases $Q_5$. The resulting voltage drop across $R_{17}$ is coupled through $C_{11}$ which reverse biases the base-emitter junction of $Q_6$.

The increased voltage drop across the common emitter resistor due to $Q_5$ being in the "on" state, aids in "turning off" $Q_6$. Because the emitter current of $Q_6$ when it is in the "on" state is greater than the "on" current of $Q_5$, the voltage across $R_{14}$ drops enough such that $Q_5$ is now kept in the "on" state by the presence of $V_{in}$. Both transistors stay in these states until the exponential discharge of $C_{11}$ through $R_{15}$ reaches a level which is slightly more positive than the voltage across $R_{14}$. This forward biases the base-emitter junction of $Q_6$ placing it

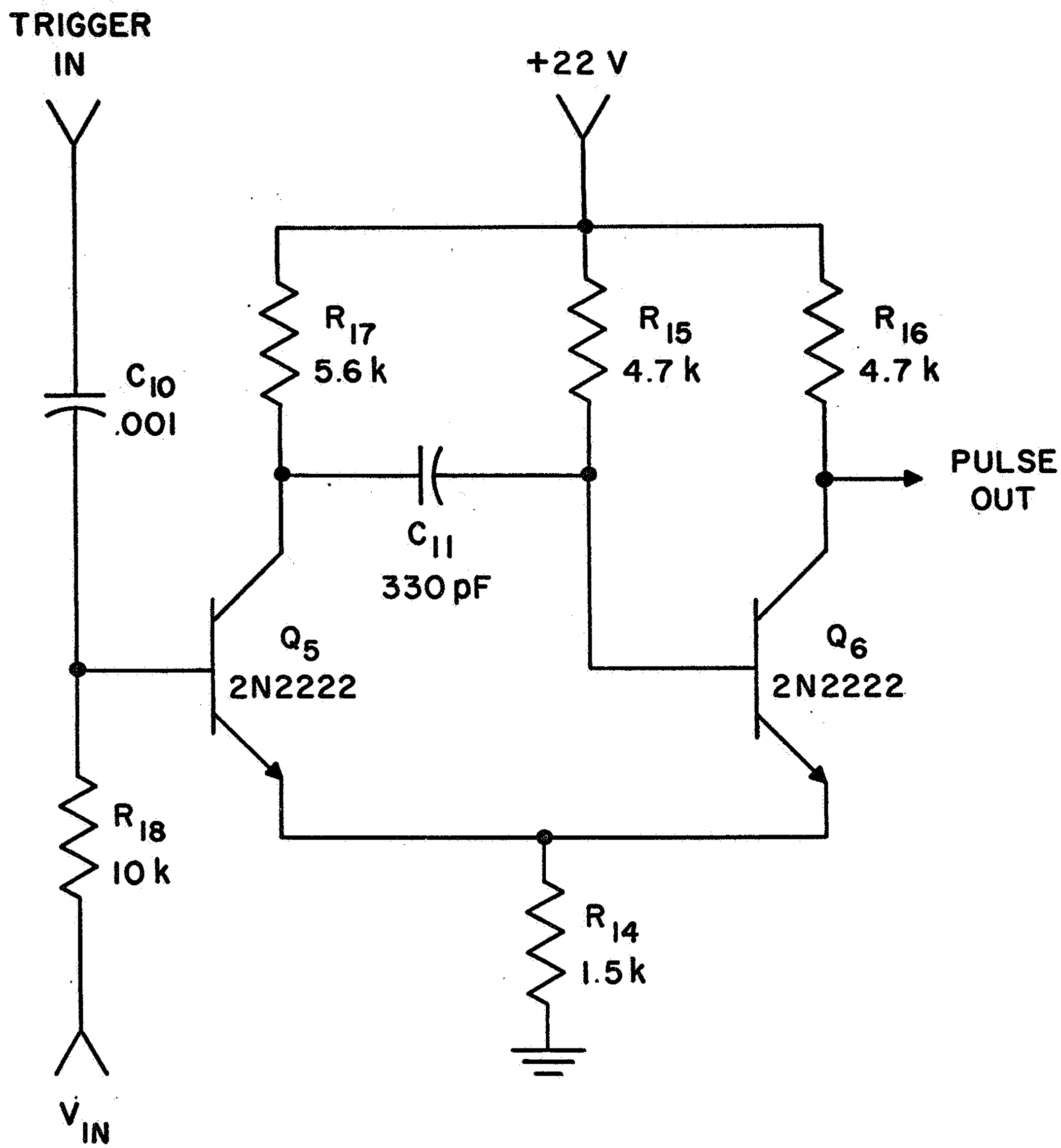


VOLTAGE CONTROLLED MONOSTABLE MULTIVIBRATOR

FIGURE 11

in the "on" state. At this point both transistors have returned to their initial states and will remain in these states until another trigger pulse occurs. Resistor $R_{18}$ is inserted in $Q_5$'s base lead so that the triggering pulse does not "see" the low output impedance of the ramp generator which supplies the voltage $V_{in}$.

Since the voltage across $R_{14}$ follows $V_{in}$ during the period when $Q_6$ is off, the output pulse duration will be exponentially related to $V_{in}$. By using a large time constant for $R_{15}$ $C_{11}$ (33 usec) compared to the required output pulse widths ($\frac{1}{2}$ to 6 usec) the relation is nearly linear over the region of interest as shown in Figure 12. The actual levels of the output waveform are 7 and 22 volts as $Q_6$ goes through its "on, off, on" cycle.

One inherent problem encountered with this circuit has been the fact that the slope of the trailing edge of the output waveform is not constant as the voltage controlled monostable multivibrator is swept through its range of pulse widths. The intention was to differentiate the trailing edge of the output waveform and use it to drive the gating stage. However the continually changing slope will produce a varying drive signal which would in turn affect the shape of the gating pulse. For this reason a comparator stage was introduced between the monostable multivibrator and the differentiator. A discussion of the comparator appears in chapter 5.

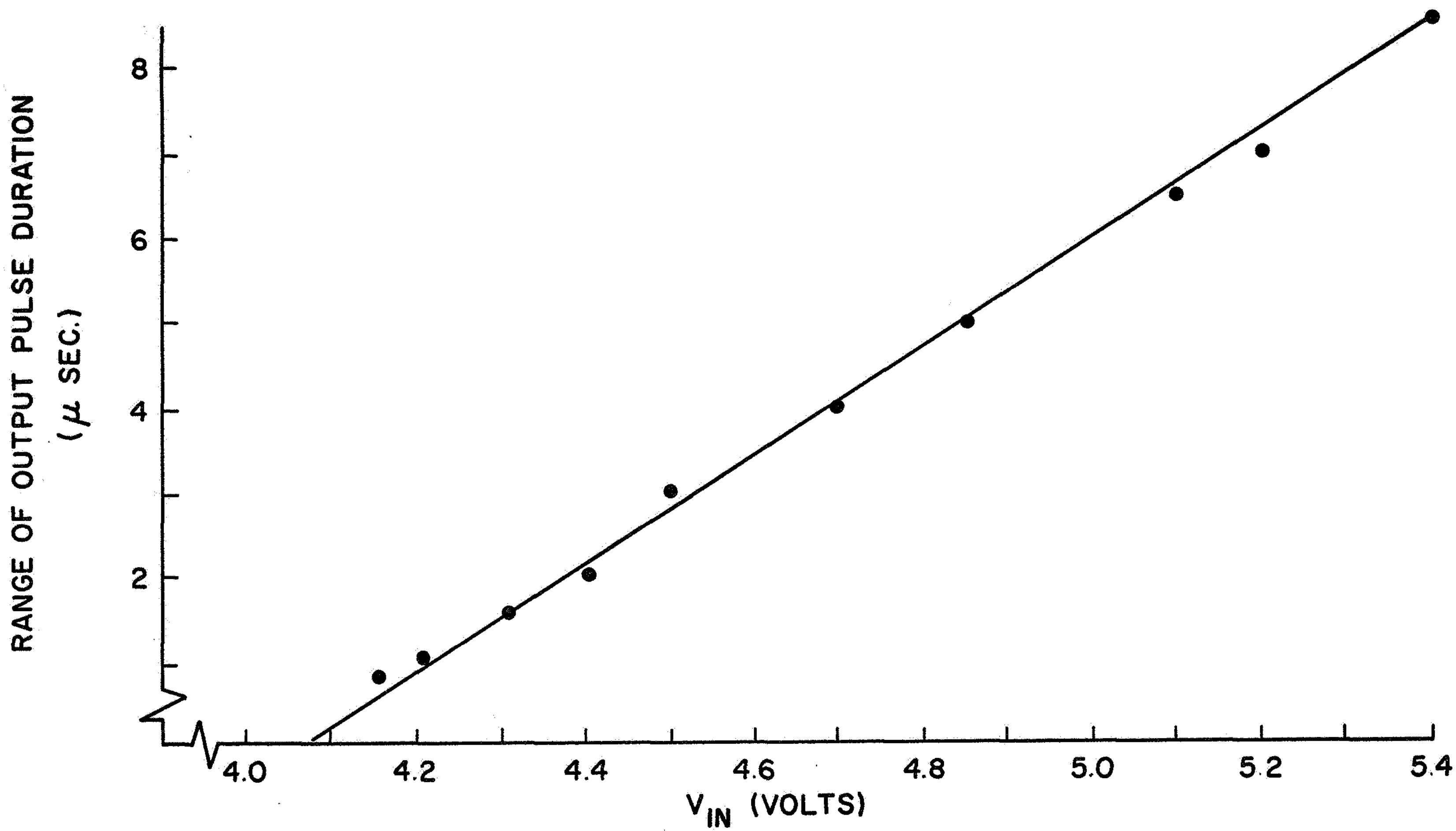


OUTPUT PULSE DURATION VS.
APPLIED VOLTAGE $V_{IN}$ TO VOLTAGE CONTROLLED MULTIVIBRATOR

FIGURE 12

## 4.2 The Ramp Function Generator

The ramp function generator used to drive the voltage controlled monostable multivibrator is shown in Figure 13. The generator is an adaptation of a previously used circuit.[7] Assume that the integrator output voltage is initially zero. Assume also that the voltage at point A is low enough such that the voltage divider action of $R_{20}$ and $R_{21}$ establishes less than 2.5 volts on the positive input of the comparator $Q_8$. The negative input of the comparator is held to +2.5 volts by $R_{22}$ and $R_{23}$ from the +15 volt supply. $C_{13}$ is used to keep the negative input insensitive to noise. The output of the comparator is then negative. This shows the second assumption to be correct for the values of $R_{20}$ and $R_{21}$ shown. The actual voltage appearing at point A is determined by the forward biased diode divider action of $D_5$, $R_{24}$ and $R_{25}$ from the -10 volt comparator output. A small portion of the output appearing at point B is integrated by $R_{19}$, $C_{12}$ and the operational amplifier $Q_7$. Because the standard inverting integrator configuration is used, the integrator's output is a positive-going ramp. With the values of $R_{19}$ and $C_{12}$ shown, the values of $R_{25}$ and $R_{26}$ were chosen to obtain a sweep time of 15 seconds for preliminary laboratory use. When the integrator output reaches +5 volts the voltage at the positive comparator input is +2.5 volts for the values of $R_{20}$ and $R_{21}$ shown and the comparator switches states. Its output and the potential at point A will then go

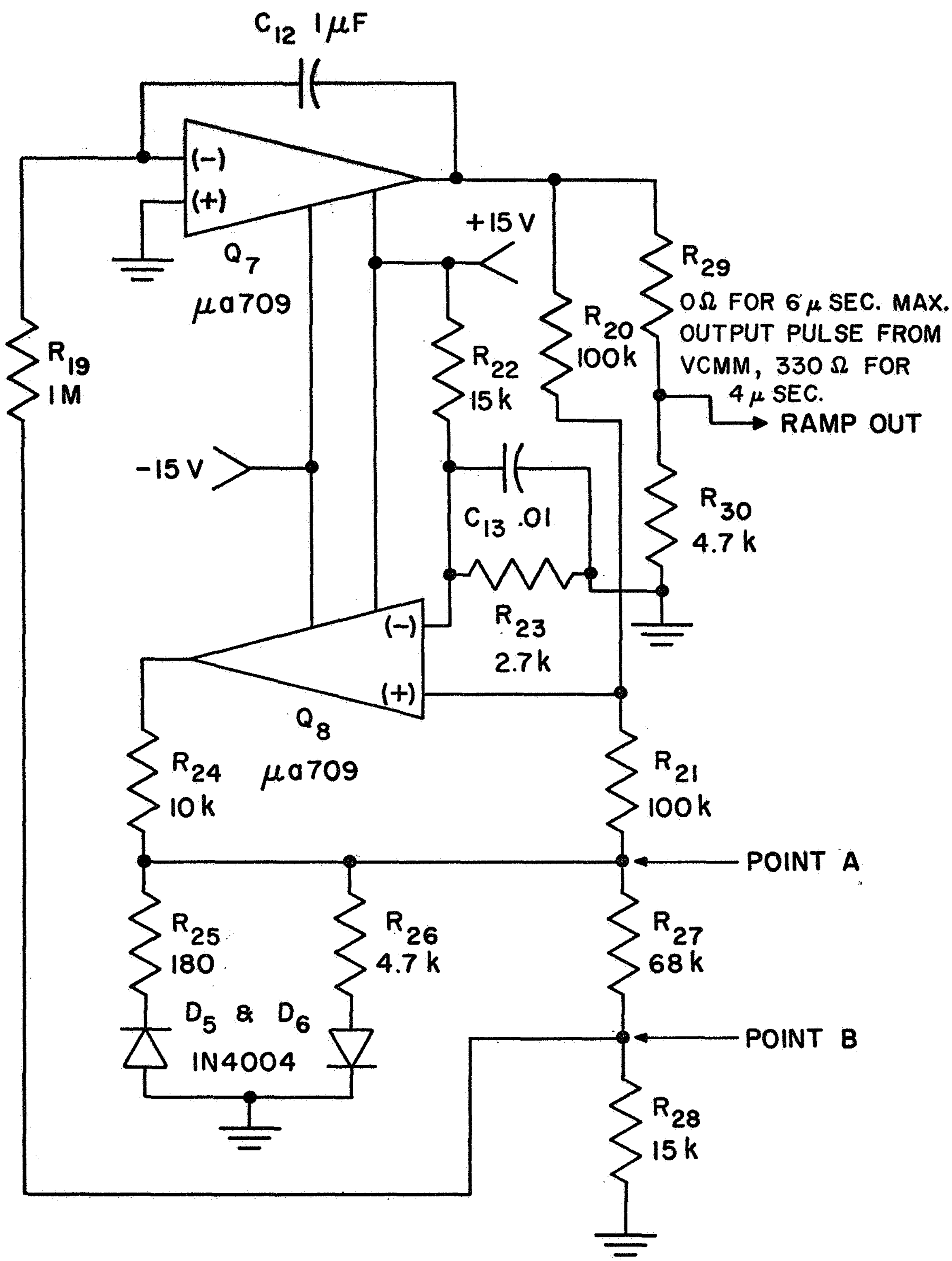


RAMP GENERATOR

FIGURE 13

positive. The integrator will then be integrating a positive potential and its ramp will approach zero, at which time the comparator will again switch states and the process is repeated. The +2.5 volts on the negative comparator input is necessary to obtain a ramp function drive to the voltage controlled monostable multivibrator which ranges from zero to +5 volts. A voltage divider, $R_{29}$, $R_{30}$, is used to set the exact upper limit of the ramp drive to the monostable multivibrator. For the values shown the maximum pulse duration from the monostable multivibrator is 6 usec. The network consisting of $R_{25}$, $R_{26}$, $D_5$, $D_6$ and $R_{24}$ determine the different positive and negative parts of the ramp.

It should be noted that the integrated circuit used for $Q_8$ (Fairchild ua709) is actually intended for operational amplifier applications. However the ua710 comparator is not desirable for this application since its output levels are 0 and +5 volts. The 709 unit has output levels of $\pm 10$ volts, allowing more versatility in adjusting the two sweep times. It was conceivable that using the ua709 as a comparator could have resulted in its "hanging-up" in saturation. However, the problem was not encountered.

CHAPTER V

# GENERATING THE GATING PULSE

## 5.1 Adding a Comparator After the VCMM

The comparator circuit used to drive the differentiator is shown in Figure 14. The particular unit used is a Fairchild ua710 integrated circuit comparator. The differential input is restricted to five volts or less. For this reason resistors $R_{31}$ and $R_{32}$ are used to reduce the 7 and 22 volt waveform levels to 0.6 and 2 volts. The reduced pulse is then applied to the negative input rather than the positive input in order to obtain the correct output pulse polarity needed to develop the negative gating pulse. The positive input is held at about +1.2 volts by the voltage divider network $R_{33}$ and $R_{34}$ from the +15 volt supply. The actual point at which the comparator changes states corresponds to a potential of 14 volts at the input to $R_{31}$. It is at this potential that the trailing edge slope has its largest value thus enabling the comparator to switch as rapidly as possible. The zener diode $D_7$ and Resistor $R_{35}$ are used to furnish the -6.8 volts required to power the comparator in addition to the +15 volts shown. The internal circuitry of the 710 comparator limits the output levels at 0 and +5 volts. With the positive and negative inputs connected as shown the output of the comparator is a negative going pulse, i.e. the output is

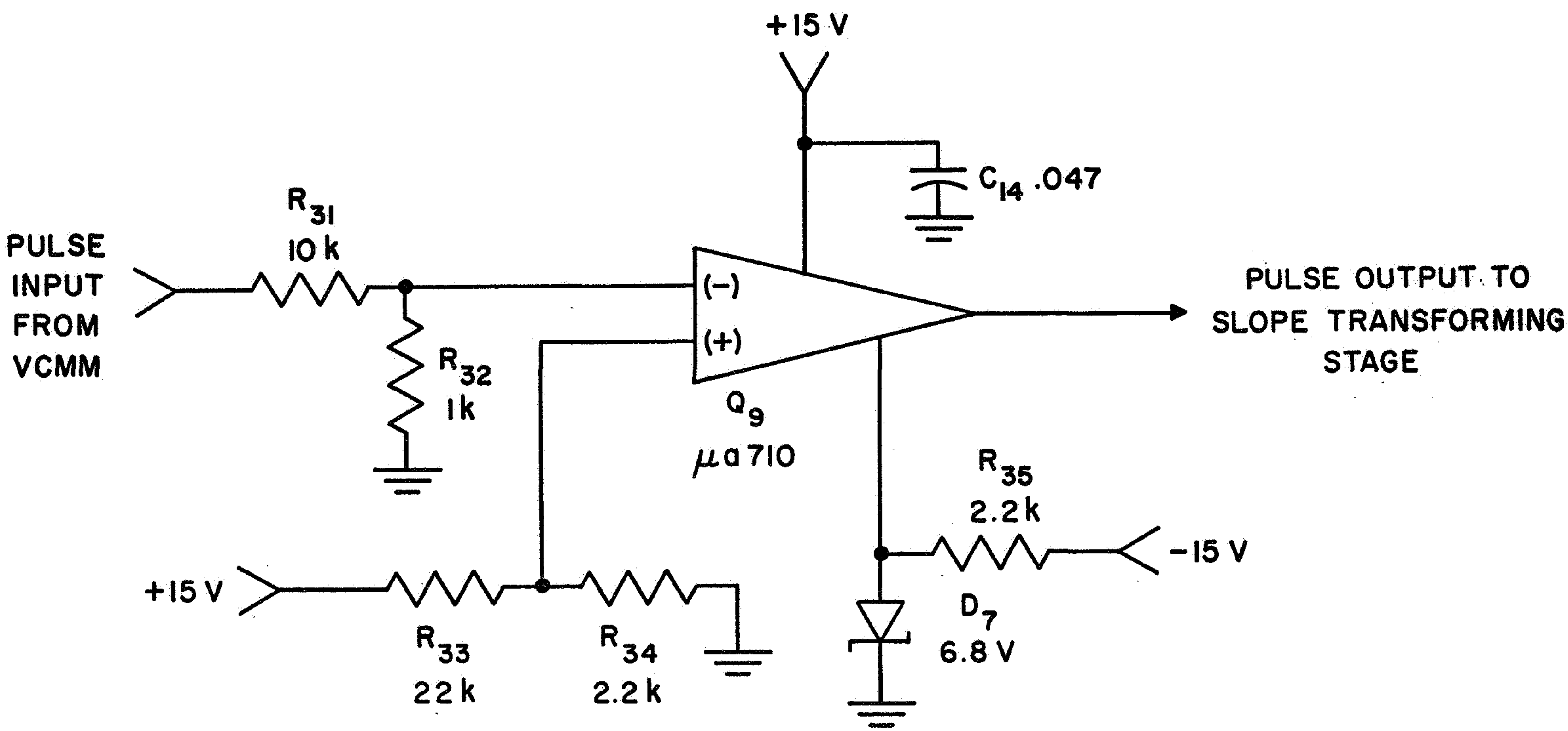


COMPARATOR STAGE

FIGURE 14

normally at +5 volts and is pulsed to 0. The slope of the trailing edge is constant and not dependent upon the pulse width, thus achieving the desired result.

## 5.2 Circuitry for Slope Transformation, Differentiation, and Amplification

The next step would normally be to differentiate the trailing edge of the comparator's output pulse and amplify it to obtain the gating pulse. However after taking the derivative of the relatively low output swing of the comparator (five volts), the level is too low to sufficiently forward bias the base-emitter junction of an amplifying stage. The approach taken then was not to differentiate but to amplify first, then differentiate. Because a differentiator presents a rather capacitive load which deteriorates the trailing edge of the pulse, the circuit shown in Figure 15 was used to transform the trailing edge of the comparator's output into a leading edge. Normally the 5 volt level from the comparator's output is attenuated by $R_{36}$ and $R_{37}$ to a level which still leaves $Q_{10}$ in a nonconducting state. A triggering pulse applied to the voltage controlled monostable multivibrator switches the comparator into an output of 0 volts as the leading edge of the monostable output is formed. The transition from 5 to 0 volts still leaves the base-emitter junction of $Q_{10}$ effectively reverse biased and $Q_{10}$ remains in the cutoff state, and the collector potential stays at

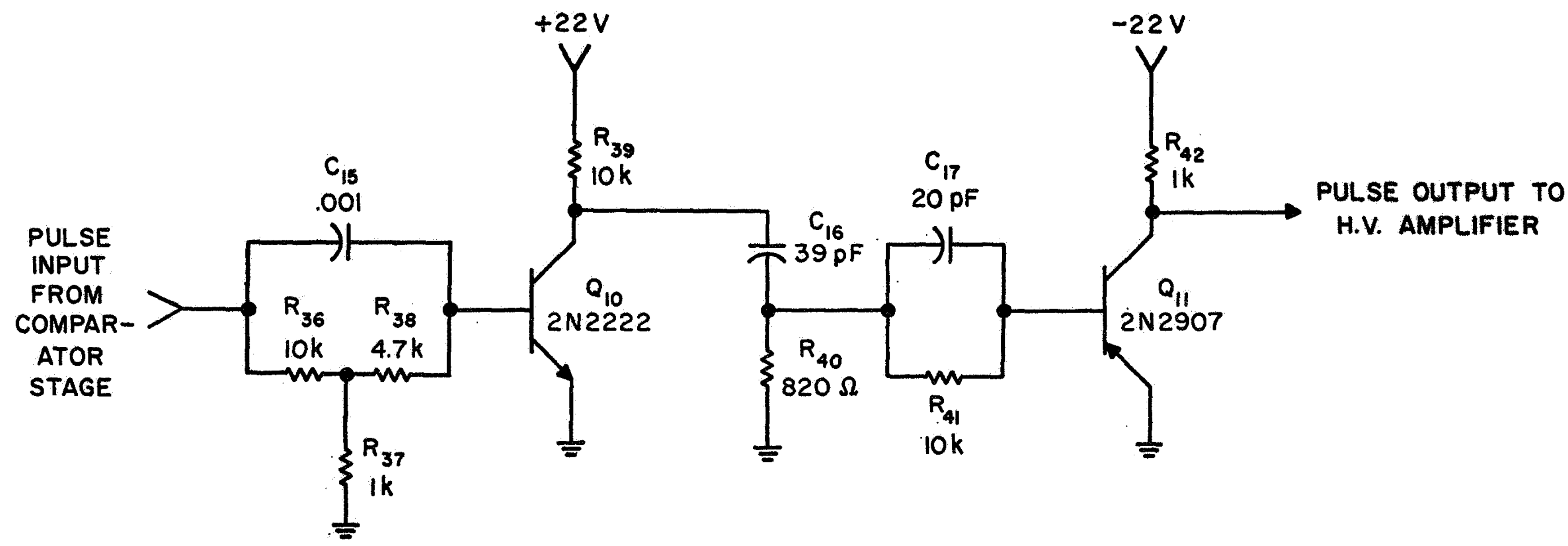


CIRCUITRY FOR SLOPE TRANSFORMATION, DIFFERENTIATION, AND AMPLIFICATION

FIGURE 15

+22 volts. However the trailing edge of the monostable output pulse after passing through the comparator stage is a positive-going waveform and is capacitively coupled through $C_{15}$, forward biasing $Q_{10}$, and driving its collector voltage to near zero volts. A rather large collector resistor, $R_{39}$ can be used since the rise time of the pulse appearing at the collector is nearly independent of the collector circuitry, thus reducing the instantaneous current demands upon the +22 volt supply. The exponential discharge of $C_{15}$ in the base circuitry determines when $Q_{10}$ again returns to cutoff. With the circuit values shown the trailing edge of the comparator's output waveform produces a voltage waveform at the collector of $Q_{10}$ which has a 25 nsec leading edge.

The differentiator network and the inverting amplifier used to drive the gating amplifier, also shown in Figure 15, are basically the same as the circuitry used to trigger the voltage controlled monostable multivibrator. However the elaborate filtering of the positive part of the derivative is not needed because the rather long trailing edge of the waveform at $Q_{10}$'s collector produces a very low amplitude derivative.

## 5.3 The Gating Amplifier

The rather large amplitude negative-going gating pulse requirement necessitates using a PNP transistor with a breakdown of 120 volts or more. The narrow pulse width requires that such a transistor be useful to 200-250 mc. At present there are no such units commercially available at a reasonable cost. A triggered blocking oscillator could be used to generate the gating pulse by using a 30 to 60 volt breakdown unit and a step-up transformer to obtain the 100 volt pulse height. The method actually used had two 250 mc 60 volt transistors connected in series similar to the common cascode circuit used with electron tubes. The circuit is shown in Figure 16. The basic idea of using transistors in series to obtain high voltage waveforms is not new, but is usually used as an amplifier by biasing the transistors at an operating point.[8] The circuit used in Figure 16 uses both transistors operating between saturation and cutoff and is therefore more usable with pulse waveforms.

Transistor $Q_{12}$ is normally in a cutoff condition. $Q_{13}$ is also at cutoff since its base and emitter are connected together through $R_{43}$. Resistors $R_{44}$ and $R_{45}$ equalize the voltage across each transistor but are large compared to $R_{46}$ so that the potential at the collector of $Q_{13}$ is nearly equal to the supply voltage.

A narrow, positive drive pulse from the previous stage, $Q_{11}$, forward biases the base-emitter junction of $Q_{11}$, "pulling" its collector voltage (and the emitter voltage of $Q_{13}$) toward ground potential. The base of $Q_{13}$ is held at a 60 volt potential due to the fact that $C_{18}$ had been charged to 60 volts during the period when both transistors

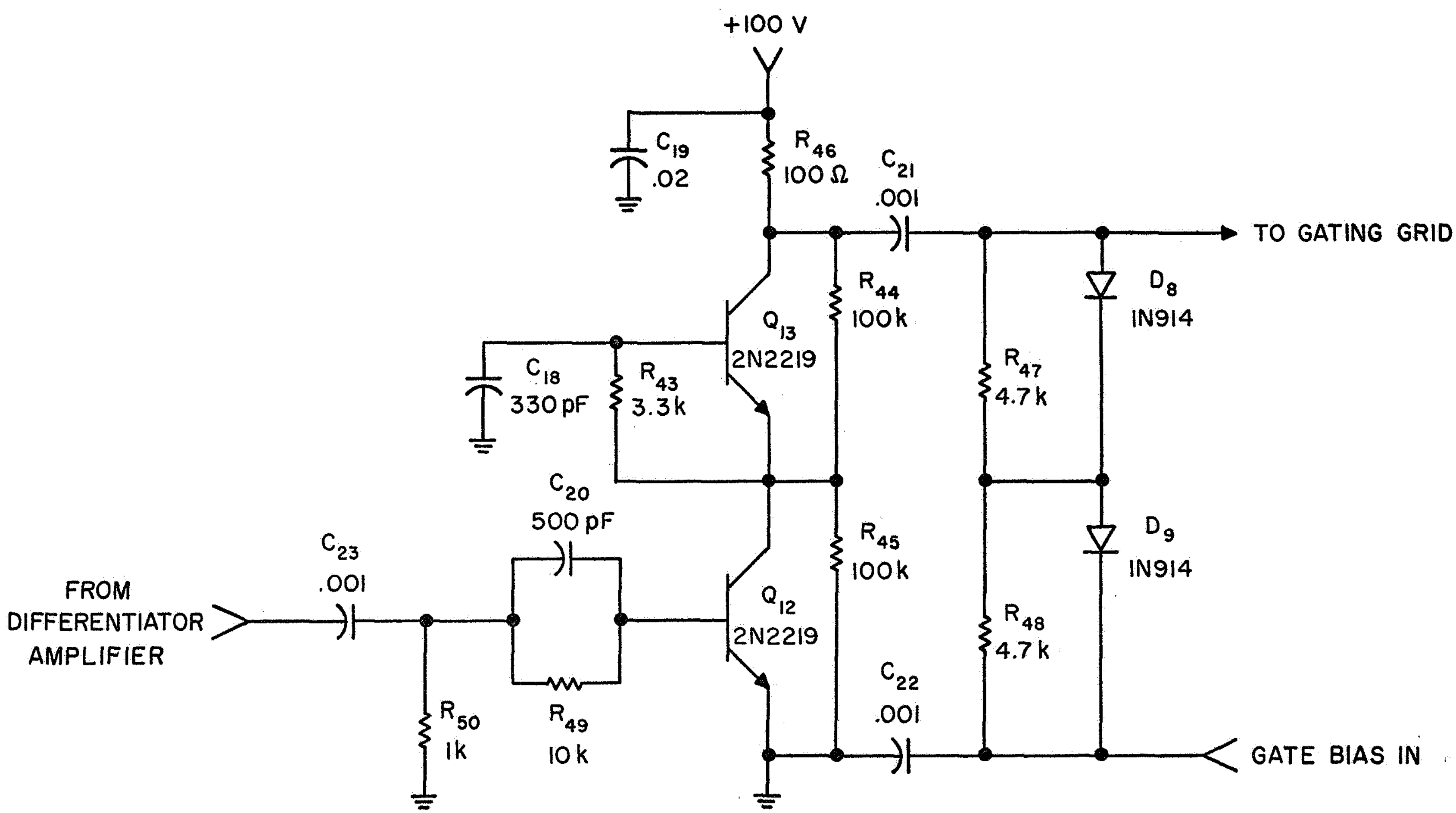


HIGH VOLTAGE GATING AMPLIFIER

FIGURE 16

were at cutoff. $Q_{13}$ is then forward biased since its base is at a higher potential than its emitter and its collector also approaches ground potential. The net result is that the two transistors act as a single unit being driven from cutoff to saturation. $C_{18}$ retains enough charge to keep $Q_{13}$ forward biased for the duration of the drive pulse.

After the drive pulse has occurred, $Q_{12}$ returns to cutoff which places $Q_{13}$ also in cutoff, thus completing the formation of a narrow, negative gating pulse at the collector of $Q_{13}$. The pulse is coupled through $C_{21}$ onto the gating grid. Bias is applied through the network consisting of $D_8$, $D_9$, $R_{47}$ and $R_{48}$, as it was for the accelerating pulse.

# CHAPTER VI

# CONCLUSIONS

## 6.1 Power Requirements

The complete block diagram and circuit diagram are shown in Figures 17 and 18. The system was powered in the laboratory by zener diodes from a common supply. The following potentials and currents were required:

+22 volts @ 10 ma
-22 volts @ 1 ma
+15 volts @ 10 ma
-15 volts @ 10 ma
+100 volts @ 2.5 ma
-85 volts @ 2.5 ma

## 6.2 Results

The mass spectrum of Figure 19 was obtained using the pulse circuitry described. The spectrum was taken by using an XY recorder and slowing down the ramp generator circuitry to several seconds to allow the recorder pen to follow the electrometer's output.

## 6.3 Summary

The clock multivibrator is the most temperature sensitive area of the circuitry. Looking upon this as being a prototype unit, a flight version should contain a temperature compensated integrated circuit clock multivibrator. As more specialized integrated circuits become available it would be advantageous to utilize them for the obvious reduced size and power requirements.

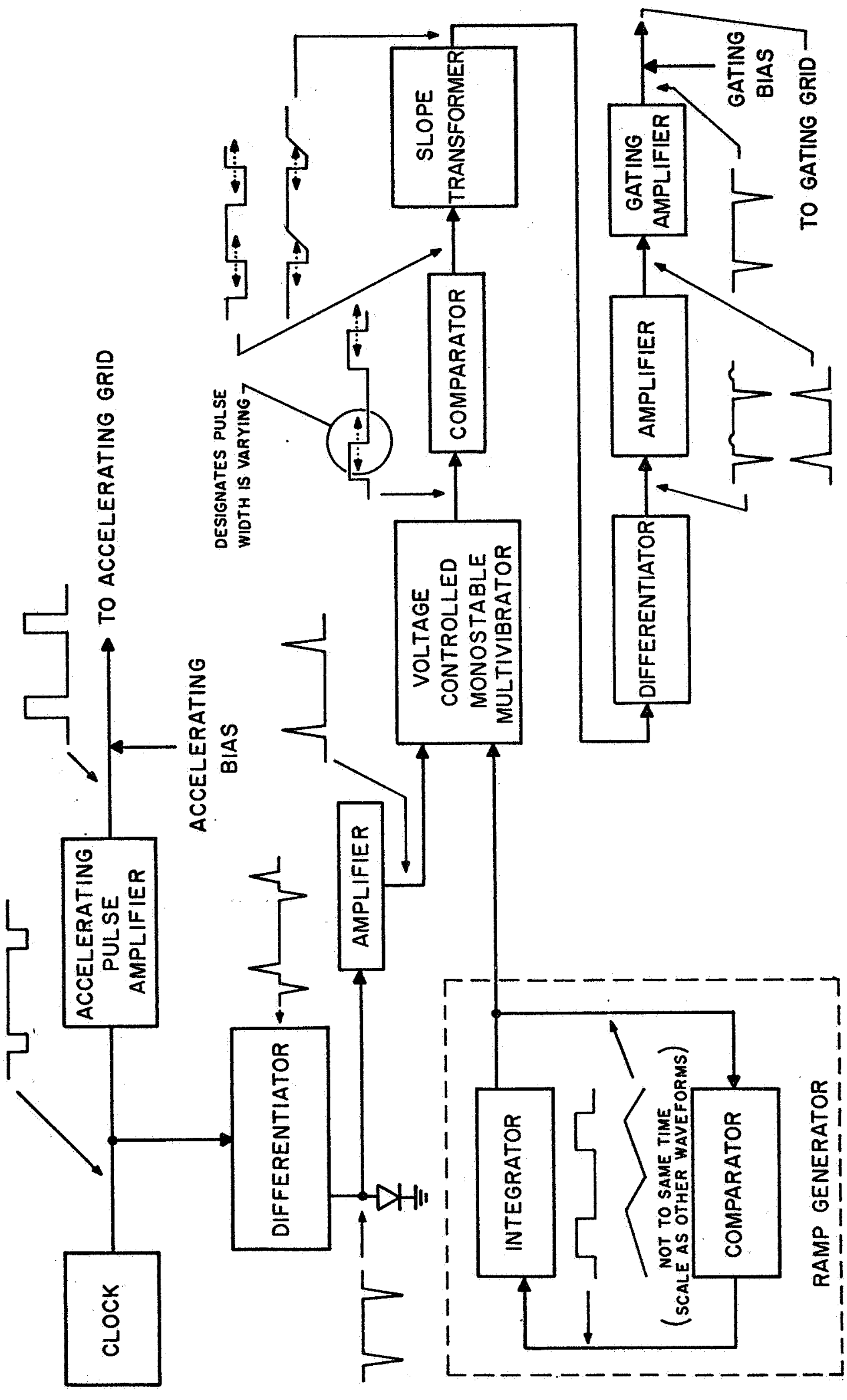


SYSTEM BLOCK DIAGRAM

FIGURE 17

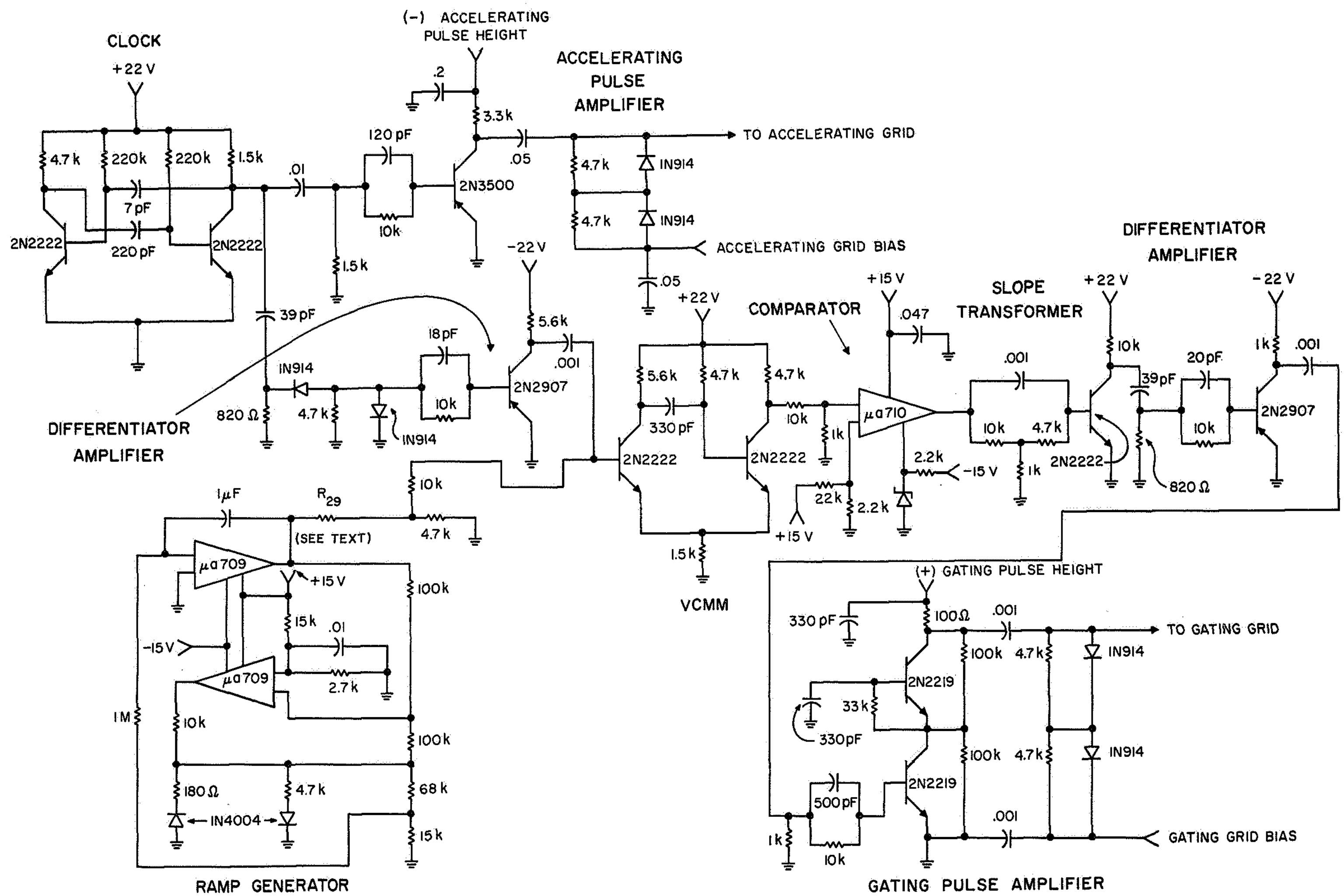


## COMPLETE SCHEMATIC DIAGRAM

FIGURE 18

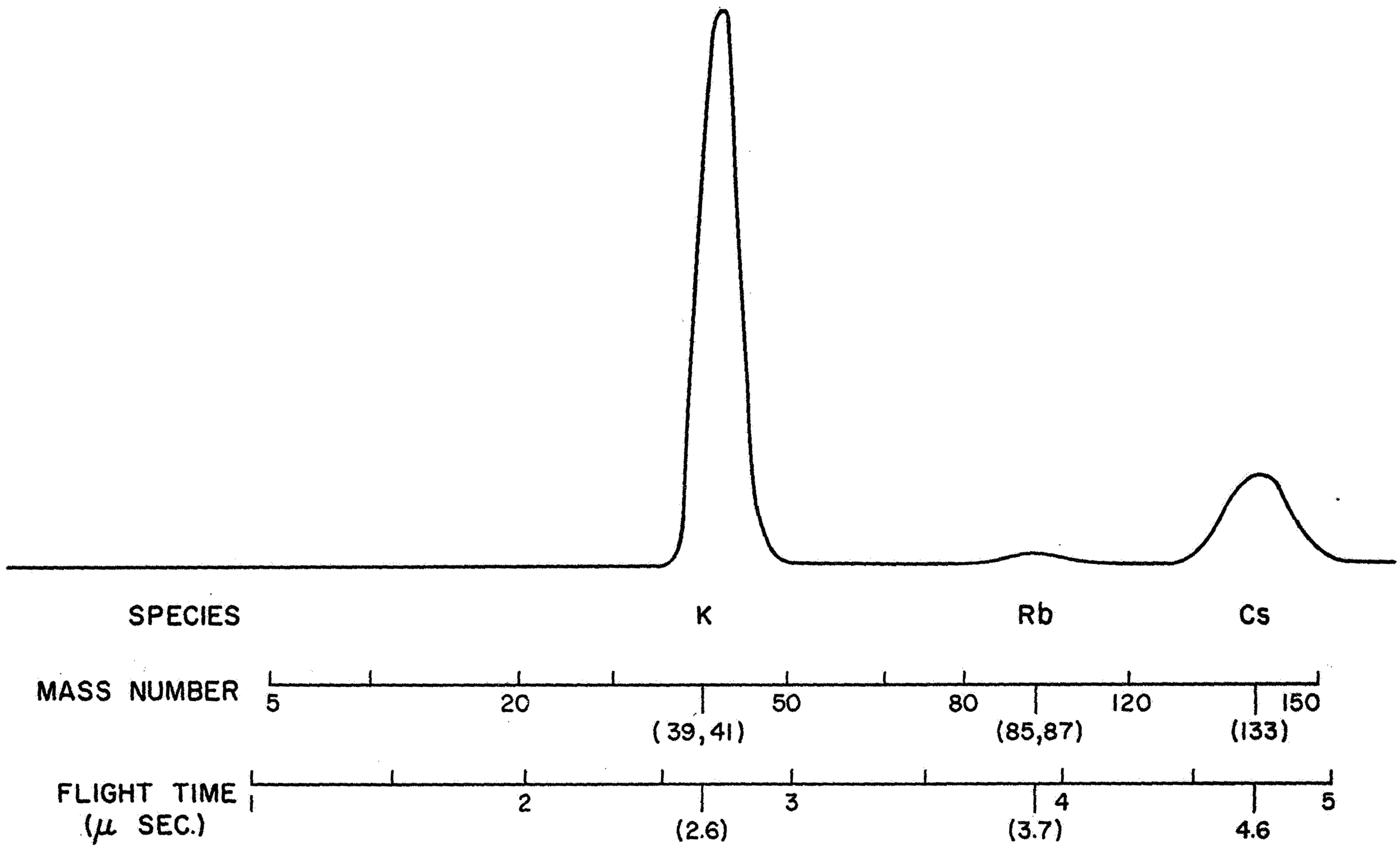


MASS SPECTRUM OBTAINED FROM WEDGE TIME-OF-FLIGHT MASS SPECTROMETER PULSE CIRCUITRY DESCRIBED IN TEXT

FIGURE 19

Possibly the most useful circuit ideas developed during this investigation which are applicable in other areas are those of sections 5.2 and 5.3. Section 5.2 utilizes the concept of taking one pulse and constructing a second pulse where the trailing edge of the first is the leading edge of the second. This technique is applicable particularly when the inherently heavy capacitive loading of a differentiator circuit deteriorates the pulse decay time. The differentiator output is then not the desired sharp spike, but one of a lower level and increased width. The pulse amplifier technique of section 5.3 enables the use of relatively low voltage, low cost, fast transistors in a series arrangement which produces high voltage pulses by using the transistors as saturated switches rather than as conventional amplifiers.

## BIBLIOGRAPHY


1. Stephens, W. E., Bull. Am. Phys. Soc., 21, 691 (1946).

2. Wiley, W. C. and McLaren, I. H., Rev. Sci. Instr. 26, 1150 (1955).

3. Diem, H. T., Scientific Report No. 309, Ionosphere Research Laboratory, Pennsylvania State University (1966).

4. Wager, J. H., J. Electronics and Control, 8, 227 (1960).

5. Katzenstein, H. S. and Friedland, S. S., Rev. Sci. Instr. 26, 324 (1955).

6. Millman, J., and Taub, H., "Pulse, Digital, and Switching Waveforms", McGraw-Hill, Inc., New York, 1965.

7. "Type O-Operational Amplifier Instruction Manual" Tektronix, Inc., Beaverton, Oregon, 1963.

8. Thornton, R. D., Searle, C. L., Pederson, D. O., Adler, R. B., and Angelo, E. J. Jr., "Semiconductor Electronics Education Committee/Volume 5", John Wiley and Sons, Inc., New York, 1965.